

Sideslip Estimation of Formula Student Prototype through GPS/INS fusion

André Antunes², Carlos Cardeira^{1,2} and Paulo Oliveira^{1,2}

¹IDMEC, ²Instituto Superior Técnico

Universidade de Lisboa, 1049-001 Lisboa, Portugal

{andre.antunes, carlos.cardeira, paulo.j.oliveira}@tecnico.ulisboa.pt

Abstract—This paper describes the design and tuning of a sideslip estimator, based on data from an inertial measurement unit (IMU), a global positioning system (GPS), wheel encoders, and from the underlying dynamic model of a car. The estimates of position, velocity, and rate gyro bias terms are also provided as by-products of the proposed methodology. A non-linear dynamic model of a car and realistic models for the sensors are both developed and implemented on a realistic simulation environment to illustrate the performance of the proposed solution. Validation on a Formula Student prototype is underway but the methodology proposed can be applied to all vehicles moving in two dimensions.

Index Terms—Navigation system, Sideslip, Kalman Filter, Sensors

I. INTRODUCTION

During the last decades, many mobile robotics competitions have been created to combine research results, engineering development and attract public audience [1]. Robocup, Darpa Challenges, FIRST LEGO League, MBZIRC are examples of such competitions that pushed forward the development of these autonomous cars. Autonomous driving are among the most popular competitions, where the robot must follow a lane [2] or navigate in unknown environments [3]. Central to this work is Formula Student, the biggest educational engineering competition, challenging university students from around the world to design and build a single-seat racing car. This competition was founded in 1980 in the U.S.A., and has been in constant evolution from standard combustion engines and tubular chassis to electric motors and composite structures. Recently, Formula Student competitions engaged in a new class for autonomous driverless cars, where the prototypes will have the same regulations as the current ones, and the track will maintain its classic outdoor racing track appearance with no special assistance for the driverless cars. These regulations raised automatic localization, guidance, control, and navigation problems that are already implemented in commercial autonomous driving cars, namely Google and Testa cars.

This paper addresses preliminary phases of autonomous driving for a Formula Student car, in particular with the identification of the sideslip of the car, resorting to global position system (GPS), an inertial measurement unit (IMU), steering encoder, and the torque from the motors. The sideslip of a car is defined as the angle between the heading of the car and the vector of velocity. Physically, is related to the

978-1-5090-6234-8/17/\$31.00 ©2017 IEEE

handling behavior of the car namely understeer, neutral steer, or oversteer. The car models presented in this work are based on a real Formula Student prototype, as depicted in Fig.1 (not driverless). This prototype is equipped with 2x50kW electric motors, with an acceleration from 0-100km/h in 2.9sec, and a top speed of 150km/h, for a weight of 280kg.

This document presents a set of three interconnected filters based on Kalman Filter (KF) and a non-linear alternative based on an Extended Kalman Filter (EKF), to give an estimation of the sideslip, where the first two are kinematic complementary filters for attitude and position already explored in [4], and the third uses a planar dynamic model of the car. A comparison between a linear model using a KF and a non-linear model using an EKF is reported.

The organization of this paper is: Section II presents the non-linear and linear planar dynamic car models, and sensor models; Section III presents the structure used at each filter and their interconnections; Section IV illustrates the operation of the solutions proposed, in simulation; Section V illustrates the operation of some of the filters for data collected in the real prototype; Finally, section VI outlines some remarks and future work.



Fig. 1. IST - FST06e at Czech Republic

II. CAR MODEL

In this section, two dynamic models are proposed that will be central to tackle the estimation problems at hand. First a non-linear model is proposed, with all the dynamics available, followed by the deduction of a commonly used linear model [5]. The first assumption for the two models is to consider only planar dynamics, and thus the assumption of no pitch (θ) or

roll (ϕ) rotation angles. This also implies that no load transfer occurs.

A. Non-linear Model

Assuming the car as a rigid body, the dynamics can be expressed by the Newton-Euler Equations of motion. Considering a reference frame attached to the centre of gravity (CG), results that:

$$F_x = m\dot{v}_x - mr v_y \quad (1a)$$

$$F_y = m\dot{v}_y + mr v_x \quad (1b)$$

$$M_z = \dot{r}_z I_z \quad (1c)$$

where r is the angular velocity around Z-axis, i.e. the yaw rate of the car, v_x and v_y are the longitudinal and transversal velocities, respectively, F_x and F_y are the longitudinal and lateral forces, m is the mass of the vehicle, and I_z is the inertia around the Z-axis. Neglecting the aerodynamic influences, the only forces acting on the car are expressed in Fig.2, all depending on the tyres. Let the tyres indexation be Front Left (FL), Front Right (FR), Rear Left (RL) and Rear Right (RR). The steering angle δ is assumed to be equal on the two front wheels.

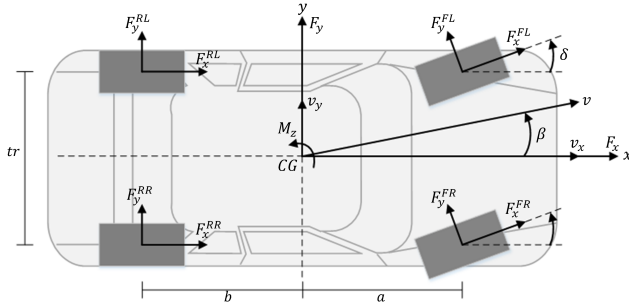


Fig. 2. Forces applied on the Car

Additionally, the following simplifications are used: $F_x^F = F_x^{FL} + F_x^{FR}$; $F_x^R = F_x^{RL} + F_x^{RR}$; $F_y^F = F_y^{FL} + F_y^{FR}$; $F_y^R = F_y^{RL} + F_y^{RR}$. Assuming the car is rear driven only, and neglecting the rolling resistance of the tyres, then $F_x^F = 0$, moreover any kind of moment created by a differential is neglected, and so $F_x^{RL} = F_x^{RR}$. Combining now the set of equations (1) with the respective forces acting on the car (Fig.2), the balance can be written as:

$$\dot{v}_x = v_y r - \frac{1}{m} [F_y^F \sin \delta - F_x^F] \quad (2a)$$

$$\dot{v}_y = -v_x r + \frac{1}{m} [F_y^F \cos \delta + F_y^R] \quad (2b)$$

$$\dot{r}_z = \frac{1}{I_z} a F_y^F \cos \delta - \frac{1}{I_z} b F_y^R \quad (2c)$$

B. Tyres

Lateral forces are generated on the tyres and depend on several parameters [6] like, tyre compound, road surface, pressure, inclination angle (IA), temperature, vertical load (F_z) and slip angle (α). Several tyre models exist, that can predict the lateral forces produced.

1) *Linear Tyre Model*: the linear approach is given by:

$$F_y = -C_\alpha \alpha_i \quad (3)$$

where C_α is the cornering stiffness that depends on α , and the subscript i is the wheel index. As seen in Fig.3, the slip of a wheel is $\alpha_i = \beta_i - \delta_i$. The sideslip of the car is defined as $\beta = \tan^{-1}(\frac{v_y}{v_x})$, knowing that a wheel is located at a distance ${}^B r_i = (x_i, y_i)$ from the car center of gravity, then the velocity components of the wheel are $v_i = {}^B v + {}^B r_i \times {}^B r_i$, and the slip of the wheel (α_i) can be expressed as:

$$\alpha_i = \tan^{-1}(\frac{v_y + x_i r}{v_x - y_i r}) - \delta_i \quad (4)$$

For the rear tyres note that $\delta_i = 0$.

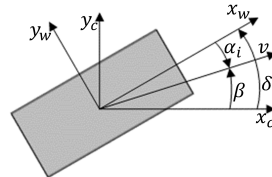


Fig. 3. Wheel vectors. The w and c suggest the wheel and car reference frames respectively, and v is the velocity vector.

The cornering stiffness presented in (3) is a linear approximation for small angles of α_i . If every tyre variable is fixed except for the tyre slip angle, then for a constant vertical load with $IA = 0$, the graph $F_y = f(SA)$ and the cornering stiffness approximation are as presented in Fig.4.

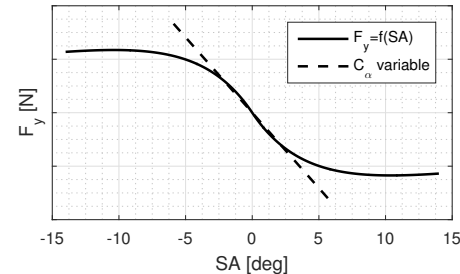


Fig. 4. Lateral force depending on slip angle. Using tyre model, and linear approximation.

It is important to remark that the limitation of this linear approximation is that it never saturates.

2) *Tyre Model*: Several tyre models have been introduced over the years like the Magic Formula of Pacejka and TMeasy [5]. Some of those are very precise at fitting experimental data, and can depend on almost every variable related with the tyre, as a consequence, they are extremely complex and computationally heavy with several coefficients that need to be calculated. For this work the Burckhardt tyre model [7] is used for its simplicity, and as a result is not that close to reality since it doesn't capture all the dynamics of the tyre, nevertheless for the objective of this work is enough.

Burckhardt starts by introducing a definition for longitudinal and lateral slips for two condition, driving and braking

	Braking	Driving	
Longitudinal slip (s_L)	$v_R \cos \alpha \leq v_W$ $\frac{v_R \cos \alpha - v_W}{v_W}$	$v_R \cos \alpha > v_W$ $\frac{v_R \cos \alpha - v_W}{v_R \cos \alpha}$	
Lateral slip (s_S)	$\frac{v_R \sin \alpha}{v_W}$	$\tan \alpha$	

where v_R is the rotational equivalent wheel velocity, and v_W is the vehicle velocity projected on the wheel. The Burckhardt model uses a combination of lateral and longitudinal slip to create a Kamm circle. This one relies on the combination of both slips (resultant wheel slip s)

$$s = \sqrt{s_L^2 + s_S^2} \quad (6)$$

On this work, longitudinal forces are considered a direct input for simplification. With this assumption is possible to combine (5) and (6) and get $s = |\tan \alpha|$.

Burckhardt methods presents an equation for friction coefficient dependent of the resulting wheel slip

$$\mu(s) = (c_1(1 - e^{-c_2 s}) - c_3 s) e^{-c_4 s \cdot v_{CG}} (1 - c_5 F_Z^2) \quad (7)$$

and five constants, where the first three are on Tab.I, parameter

TABLE I
PARAMETER SETS FOR FRICTION COEFFICIENT (BURCKHARDT)

	c_1	c_2	c_3
Asphalt, dry	1.2801	23.99	0.52
Asphalt, wet	0.857	33.822	0.347
Concrete, dry	1.1973	25.168	0.5373
Cobblestones, dry	1.3713	6.4565	0.6691
Cobblestones, wet	0.4004	33.7080	0.1204
Snow	0.1946	94.129	0.0646
Ice	0.05	306.39	0

c_4 is the velocity (v_{CG}) adjust parameter that is said to be between 0.002 s/m and 0.004 s/m . The c_5 is the vertical load and is introduced as close to $0.00015 (1/kN)^2$. The lateral force F_y is then given by the Coulomb friction equation $\mu(s) = F_y/F_z$.

In this work, the influence of velocity in the $\mu(s)$ is neglected for simplification. This method is, as explained before, discrepant from reality, but an acceptable approximation of the tyres behaviour, moreover this method is inadequate for fast dynamics in the tyre slip angle, but more convenient for a quasi-static operating point.

C. Linear Car Model

The linear model, that has been widely adopted [5][8][9], comes from the bicycle model in equations (2), and assumes both a constant forward speed ($v_x = \text{const}$) and small angle approximation. This model uses the linear tyre model (3), where the wheel slip (4), due to the bicycle model is approximated to:

$$\alpha_i = \operatorname{tg}^{-1}\left(\frac{v_y + x_i r}{v_x - y_i r}\right) - \delta_i \approx \frac{v_y + x_i r}{v_x} - \delta_i$$

Using v_y and r as state variables and δ as input, the linear model can be written in a state space form:

$$\begin{bmatrix} \dot{v}_y \\ \dot{r} \end{bmatrix} = \begin{bmatrix} -\frac{C_{\alpha f} + C_{\alpha r}}{v_x m} & -\frac{a C_{\alpha f} + b C_{\alpha r}}{v_x m} - v_x \\ -\frac{a C_{\alpha f} + b C_{\alpha r}}{I_z v_x} & -\frac{a^2 C_{\alpha f} - b^2 C_{\alpha r}}{I_z v_x} \end{bmatrix} \begin{bmatrix} v_y \\ r \end{bmatrix} + \begin{bmatrix} \frac{C_{\alpha f}}{m} \\ \frac{a C_{\alpha f}}{I_z} \end{bmatrix} \delta \quad (8)$$

D. Sensor Modelling

After the previous models, the non-linear (2) and the linear (8), it is necessary to recreate the sensors on-board the vehicle.

1) *Compass*: The compass gives the heading of the vehicle and can be easily recreated as $\psi_k = \psi + w_{\psi k}$, where ψ is the actual heading value, $w_{\psi k}$ is noise associated to the measure, and ψ_k is the measurement at instant k .

2) *Rate Gyro*: The rate gyro is directly given by $\dot{\psi}_k = r + w_{\dot{\psi} k}$, where $w_{\dot{\psi} k}$ is noise, and since the model is just planar only the angular velocity around the z-axis (yaw rate) is measured.

3) *GPS*: The GPS receiver provides positioning data expressed in a fixed coordinate frame, e.g. latitude and longitude. As an alternative, in this work the ENU (east-north-up) coordinate system is used to present a position already in usable units (meters).

4) *Accelerometer*: The accelerometer model is given by $a_r = \frac{d^B v}{dt} + \omega \times {}^B v + w_r$, where w_r is noise associated to the measurement.

III. ESTIMATOR ARCHITECTURE

In this section, the proposed architecture for the estimation of the sideslip of the car and the required measurements are presented. As depicted in Fig.5, the architecture is composed by an Attitude Complementary Filter (ACF) in order to estimate the heading of the car. Then, using this estimate in the Position Complementary Filter (PCF), the velocity components in the body frame are estimated. The Car Estimation

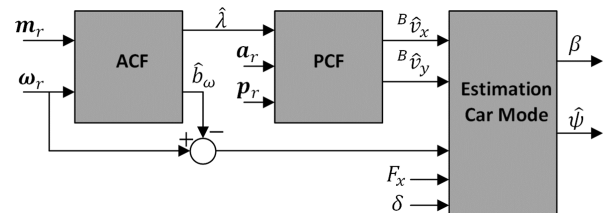


Fig. 5. Flowchart of Filter Scheme where m_r , ω_r , a_r , and p_r , are respectively the reading from the magnetometer, rate gyro, accelerometer and GPS

Model uses estimates of the velocities and the corrected yaw rate to estimate the sideslip. Also the steering angle and the longitudinal force are used, although it is assumed as available. Two models are compared for the car model, one based on a Linear Model, thus leading to the design of a Kalman Filter [10], and a non-linear model that requires the use of an Extended Kalman Filter [11]. Both complementary filters are implemented as discrete Kalman Filters and explained in detail, as a specialization of the work by [4] from 6dof to 3dof.

A. Attitude Complementary Filter

Defining $\bar{\lambda} = [\bar{\phi} \quad \bar{\theta} \quad \bar{\psi}]^T$ as the vector of attitude that contains the rotation around de X-Y-Z respectively roll, pitch and yaw, and being the $\dot{\bar{\lambda}} = \bar{\omega}$ the vector with the corresponding angular velocities, is then possible and easily interpreted the following equation:

$$\bar{\lambda}_{k+1} = \bar{\lambda}_k + T\bar{\omega}_k \quad (9)$$

where index k defines the instant in time $t = kT$ and T the sampling interval. Angular velocity is measured by a rate gyro, affected by zero-mean, Gaussian white noise $w_{\omega_r,k} \sim \mathcal{N}(0, \Xi_\omega)$ and a bias \bar{b}_{ω_k} also driven by Gaussian white-noise $w_{bk} \sim \mathcal{N}(0, \Xi_b)$

$$\omega_{rk} = \bar{\omega}_k + \bar{b}_{\omega_k} + w_{\omega_r,k} \quad (10)$$

$$\bar{b}_{\omega k+1} = \bar{b}_{\omega k} + w_{bk} \quad (11)$$

Assuming that the INS axis are perfectly aligned with the vehicle axis or that the rotation has already been made, the equations (9-11) can be rewritten in a state-space form

$$\begin{bmatrix} \bar{\psi}_{k+1} \\ \bar{b}_{\psi k+1} \end{bmatrix} = \begin{bmatrix} 1 & -T \\ 0 & 1 \end{bmatrix} \begin{bmatrix} \bar{\psi}_k \\ \bar{b}_{\psi k} \end{bmatrix} + \begin{bmatrix} T \\ 0 \end{bmatrix} \dot{\psi}_{k+} \begin{bmatrix} -T & 0 \\ 0 & 1 \end{bmatrix} \begin{bmatrix} w_{\omega_r,k} \\ w_{bk} \end{bmatrix}$$

Consider the following filter for the Newton-Euler kinematics presented before and the update equation for estimated states using Kalman Filter.

$$\begin{bmatrix} \bar{\psi}_{k+1} \\ \bar{b}_{\psi k+1} \end{bmatrix} = \begin{bmatrix} 1 & -T \\ 0 & 1 \end{bmatrix} \begin{bmatrix} \bar{\psi}_k \\ \bar{b}_{\psi k} \end{bmatrix} + \begin{bmatrix} T \\ 0 \end{bmatrix} \dot{\psi}_{k+} \begin{bmatrix} K_1 \\ K_2 \end{bmatrix} (y_k - \hat{y}_k)$$

$$\hat{y}_k = \hat{\psi}_k, \quad y_k = \bar{\psi}_k + v_k$$

where y_k is the state estimated and \hat{y}_k is the observed state corrupted by noise v_k , in this case is the heading ψ_k given by the compass. K_1 and K_2 are the feedback gains. For the calculation of the Kalman Gain, the following linear time invariant system is used

$$\begin{bmatrix} x_{\psi k+1} \\ x_{bk+1} \end{bmatrix} = \begin{bmatrix} 1 & -T \\ 0 & 1 \end{bmatrix} \begin{bmatrix} x_{\psi k} \\ x_{bk} \end{bmatrix} + \begin{bmatrix} -T & 0 \\ 0 & 1 \end{bmatrix} \begin{bmatrix} w_{\omega k} \\ w_{bk} \end{bmatrix} \quad (12a)$$

$$y_{xk} = [1 \quad 0] \begin{bmatrix} x_{\psi k} \\ x_{bk} \end{bmatrix} + v_{\psi k} \quad (12b)$$

B. Position Complementary Filter

The Position Complementary filter relies on position and acceleration measurements to estimate the velocity. This one uses the GPS in the earth frame $\{E\}$ and the accelerometer in the body frame $\{B\}$. Let $\bar{\mathcal{R}}_k$ be the rotation matrix that makes the transformation from $\{B\}$ to $\{E\}$ frames. Defining $\bar{\mathbf{p}}$ as the vector which contains the position, $\bar{\mathbf{v}}$ as the vector of velocity and $\bar{\mathbf{a}}$ the acceleration vector, where the three are in the earth frame $\{E\}$, and with the assumption of planar model $\bar{\mathbf{p}}, \bar{\mathbf{v}}, \bar{\mathbf{a}} \in \mathbb{R}^2$, also ${}^B\bar{\mathbf{a}}$ can be defined as the acceleration vector in the body frame. Considering the continuous-time kinematics $\dot{\bar{\mathbf{p}}} = \bar{\mathbf{v}}$, $\dot{\bar{\mathbf{v}}} = \bar{\mathbf{a}}$, and $\dot{\bar{\mathbf{v}}} = \bar{\mathcal{R}} {}^B\bar{\mathbf{a}}$, is then possible to derive

the discrete-time equivalent that represents the equations of motion

$$\bar{\mathbf{p}}_{k+1} = \bar{\mathbf{p}}_k + T\bar{\mathbf{v}}_k + \frac{T^2}{2} \bar{\mathcal{R}}_k {}^B\bar{\mathbf{a}} \quad (13a)$$

$$\bar{\mathbf{v}}_{k+1} = \bar{\mathbf{v}}_k + T\bar{\mathcal{R}}_k {}^B\bar{\mathbf{a}} \quad (13b)$$

since no vertical axis is used, or roll and pitch, then the readings from the INS are assumed as independent of gravitational acceleration interferences. Hence is possible to rewrite the equations (13) in a state space form recalling also the GPS and accelerometer modelling described in Section II-D.

$$\begin{bmatrix} \bar{\mathbf{p}}_{k+1} \\ {}^B\bar{\mathbf{v}}_{k+1} \end{bmatrix} = \begin{bmatrix} I & T\bar{\mathcal{R}}_k \\ 0 & I \end{bmatrix} \begin{bmatrix} \bar{\mathbf{p}}_k \\ {}^B\bar{\mathbf{v}}_k \end{bmatrix} + \begin{bmatrix} \frac{T^2}{2}\bar{\mathcal{R}}_k \\ TI \end{bmatrix} \bar{\mathbf{a}}_k + \begin{bmatrix} I & -\frac{T^2}{2}\bar{\mathcal{R}}_k \\ 0 & -TI \end{bmatrix} \begin{bmatrix} w_{pk} \\ w_{ar k} \end{bmatrix} \quad (14)$$

where ${}^B\bar{\mathbf{v}}_k$ is the velocity vector expressed in the body frame, w_{pk} and $w_{ar k}$ are the noise introduced before for the sensors and $I \in \mathbb{R}^2$ is the identity matrix. Using (14), the PCF proposed filter is:

$$\begin{bmatrix} \hat{\mathbf{p}}_{k+1} \\ {}^B\hat{\mathbf{v}}_{k+1} \end{bmatrix} = \begin{bmatrix} I & T\bar{\mathcal{R}}_k \\ 0 & I \end{bmatrix} \begin{bmatrix} \hat{\mathbf{p}}_k \\ {}^B\hat{\mathbf{v}}_k \end{bmatrix} + \begin{bmatrix} \frac{T^2}{2}\bar{\mathcal{R}}_k \\ TI \end{bmatrix} \bar{\mathbf{a}}_k + \begin{bmatrix} K_{1p} \\ \bar{\mathcal{R}}_k' K_{2p} \end{bmatrix} (y_{pk} - \hat{y}_{pk})$$

$$\hat{y}_{pk} = \hat{\mathbf{p}}_k, \quad y_{pk} = \bar{\mathbf{p}}_k + \mathbf{v}_{pk}$$

where K_{1p} and K_{2p} are the feedback gains identified with the Kalman gains for the system

$$\begin{bmatrix} \mathbf{x}_{pk+1} \\ \mathbf{x}_{vk+1} \end{bmatrix} = \begin{bmatrix} I & TI \\ 0 & I \end{bmatrix} \begin{bmatrix} \mathbf{x}_{pk} \\ \mathbf{x}_{vk} \end{bmatrix} + \begin{bmatrix} I & -\frac{T^2}{2}I \\ 0 & -TI \end{bmatrix} \begin{bmatrix} \mathbf{w}_{pk} \\ \mathbf{w}_{vk} \end{bmatrix} \quad (15a)$$

$$\mathbf{y}_{xk} = [I \quad 0] \begin{bmatrix} \mathbf{x}_{pk} \\ \mathbf{x}_{vk} \end{bmatrix} + \mathbf{v}_{pk} \quad (15b)$$

C. Linear Model estimation

The Linear Model is based on equation (8). This system is function of two state variable $[v_y \quad r]$ and the state transition matrix is time-variant due to v_x . Both velocities v_x and v_y can be acquired through the Position Complementary Filter, and r is the gyro reading with the bias correction from the ACF. Since it is possible to access every variable for this system, the output matrix can be defined as $C = \begin{bmatrix} 1 & 0 \\ 0 & 1 \end{bmatrix}$.

Then, based on the system in (8), the underlying model for the estimator design is expressed as

$$\begin{bmatrix} \dot{x}_{vy} \\ \dot{x}_r \end{bmatrix} = \begin{bmatrix} -\frac{C_{\alpha f} + C_{\alpha r}}{v_x m} & \frac{-aC_{\alpha f} + bC_{\alpha r}}{v_x m} - v_x \\ \frac{-aC_{\alpha f} + bC_{\alpha r}}{I_z v_x} & \frac{-a^2 C_{\alpha f} - b^2 C_{\alpha r}}{I_z v_x} \end{bmatrix} \begin{bmatrix} x_{vy} \\ x_r \end{bmatrix} \quad (16a)$$

$$+ \begin{bmatrix} 1 & 0 \\ 0 & 1 \end{bmatrix} \begin{bmatrix} \mathbf{w}_{vy} \\ \mathbf{w}_r \end{bmatrix}$$

$$y_l = \begin{bmatrix} 1 & 0 \\ 0 & 1 \end{bmatrix} \begin{bmatrix} x_{vy} \\ x_r \end{bmatrix} + \begin{bmatrix} \mathbf{v}_{vy} \\ \mathbf{v}_r \end{bmatrix} \quad (16b)$$

In this system, the steering input δ is considered a disturbance that can also be measured. On the dynamics of this system,

two details should carefully be discussed. The first is the longitudinal velocity, if the car is stopped, every entry will be dividing by zero and cause the system to fail. The second problem is to assume a car with a perfect 50% – 50% weight distribution with four equal tyres. This situation implies that $aC_{\alpha f} = bC_{\alpha r}$ and $a^2C_{\alpha f} = b^2C_{\alpha r}$, and therefore the second line of the state transition matrix of (16) will be zero. Also is easy to conclude that the system will always be fully observable, a requirement for the Kalman Filter. Is then possible to assume that the system can't be used only for $v_x = 0$, i.e the car is not moving.

The linear time variant estimator is:

$$\begin{aligned} \begin{bmatrix} \dot{\hat{v}}_y \\ \dot{\hat{r}} \end{bmatrix} &= \begin{bmatrix} -\frac{C_{\alpha f} + C_{\alpha r}}{v_x m} & \frac{-aC_{\alpha f} + bC_{\alpha r}}{v_x m} - v_x \\ \frac{-aC_{\alpha f} + bC_{\alpha r}}{I_z v_x} & \frac{-a^2C_{\alpha f} - b^2C_{\alpha r}}{I_z v_x} \end{bmatrix} \begin{bmatrix} \hat{v}_y \\ \hat{r} \end{bmatrix} \\ &+ \begin{bmatrix} \frac{C_{\alpha f}}{m} \\ \frac{aC_{\alpha f}}{I_z} \end{bmatrix} \delta + \begin{bmatrix} K_{1v_y} & K_{1r} \\ K_{2v_y} & K_{2r} \end{bmatrix} (y_l - \hat{y}_l) \\ \hat{y}_l &= \begin{bmatrix} \hat{v}_y \\ \hat{r} \end{bmatrix}, \quad y_l = \begin{bmatrix} v_y \\ r \end{bmatrix} + \begin{bmatrix} \mathbf{v}_{v_y} \\ \mathbf{v}_r \end{bmatrix} \end{aligned}$$

where \mathbf{v}_{v_y} and \mathbf{v}_r are zero-mean, Gaussian white noise, \hat{y}_l is the estimated state vector of the linear model, and y_l is the vector that contains the most recent values of v_y from the Position Complementary Filter and r from the rate gyro with bias correction. The K_i gains are the Kalman gains that relate the error of measured and estimated data to each state variable.

D. Non-Linear Model estimation

The estimation using the non-linear model is tackled resorting to an Extended Kalman Filter. Both methods are very similar regarding the implementation, with the difference where A and B matrices are replaced with the Jacobian of the non-linear equations (2). This method uses the longitudinal velocity v_x as well as a state variable, and the state variable vector of the system is $\hat{x}_k = [v_x \quad v_y \quad r]^T$.

The output matrix for the EKF is an 3×3 identity matrix, the estimated variable is the same as the measured one.

A major difference and difficulty in the EKF is the F matrix since it's the jacobian of (2), where the lateral forces F_y on the tyres are calculated with the Burckhardt method (7), and the tyre slip angle α is calculated with (4), that depends on the three state variables. This matrix is not presented here due to its size and complexity.

IV. SIMULATION AND RESULTS

This section starts by presenting the values used for both the models and filters, followed by some case studies and a comparison between the value simulated by the dynamic car model, the estimation using the Kalman Filter and the estimation using the Extended Kalman Filter. The linear car model only uses the linear tyre model and the non-linear car model only uses the Burckhardt method. The objective of filtering and estimate states of the presented system is to feed the control system, and therefore the update frequency must

be chosen high enough to be useful for the control system but also close to the sensor frequency. With that in mind an update rate of $100Hz$ is defined which represents a sampling time of $T = 0.01s$. The fact that GPS receivers work at lower frequencies is acknowledged, and even though higher frequency systems exists, these are discarded due to high costs. Some works present multi-rate filters for situations like this, but since implementation is not the concern of this document, those techniques are left unexplored.

A. Car Values and Sensors

For the simulations ahead a reference car is defined with the following parameters withdrawn from a real Formula Student car (Fig.1) for the theoretical non-linear model (2).

TABLE II
 PARAMETERS FOR THE MODEL BASED ON REAL FORMULA STUDENT CAR

Description	Var.	Value	Units
Wheelbase	—	1.59	m
Front and Rear Track	—	1.24	m
Mass of Car + Driver	m	356	kg
Yaw inertia	I_z	120	$kg.m^2$
Weight Distribution (Front-Rear)	—	45.1 – 54.9	% – %

From these parameters is possible to derive others more useful for the model, assuming static load and a perfectly balanced left-right CG.

TABLE III
 PARAMETERS DERIVED FROM THE REAL CAR FOR THE MODEL

Description	Var.	Value	Units
Dist. from CG to front track	a	0.873	m
Dist. from CG to rear track	b	0.717	m
Half Track	tr	0.62	m
Static load at front wheel	F_F_z	787.5	N
Static load at rear wheel	R_F_z	958.7	N
Cornering Stiffness front	$C_{\alpha f}$	1.527×10^4	N/rad
Cornering Stiffness rear	$C_{\alpha r}$	1.995×10^4	N/rad

For the non-linear tyre model in section II-B2 is used the coefficients for dry asphalt of Table I on (7) with the static load of each wheel (Table III). Since in the Burckhardt model the first part of the tyre response curve is not completely linear, the cornering stiffness can't be obtained directly, instead a curve fitting is used for a slip $s \leq 0.06rad$. Using this method, for the two loading cases, front and rear, two cornering stiffness values are extracted and presented in Table III, which are a commitment between how close they are from the non-linear tyre curve and the range of α where they are valid.

To simulate the sensors on the car, zero-mean, Gaussian white noise is added to the readings, which has the characteristics on Table IV for each sensor.

Only the gyroscope is assumed to also suffer from a constant bias of 0.02 rad.

B. Filters

This sections presents the values and some properties of the filters used for the simulations ahead. The attitude and position

TABLE IV
NOISE CHARACTERISTICS AT THE SENSORS

	Units	Std	3σ	σ^2
GPS	m	0.10	0.30	0.01
Accelerometer	m/s^2	0.11	0.33	0.01
Rate Gyro	deg/s	0.51	1.53	0.26
Compass	deg	2.22	6.66	4.95

complementary filters respectively, (12) and (15), can be easily rewritten in a compact discrete state-space form as

$$\mathbf{x}_{k+1} = F\mathbf{x}_k + G\mathbf{w}_k, \quad \mathbf{y}_k = H\mathbf{x}_k + \mathbf{v}_k$$

It is also obvious from the definition of observability and controllability that both systems, ACF and PCF, are completely observable, and completely state controllable, conditions required for using the Kalman filter. Using the statistical values of Table IV as starting point, the identified weights and gains for each filter are presented in Table V.

TABLE V
COMPLEMENTARY FILTER PARAMETERS

	State Weights	Observation Weight	Kalman Gain
Attitude Filter	$\Xi_\omega = 1 \times 10^{-4}$ $\Xi_b = 1 \times 10^{-5}$	$\Theta_\lambda = 10$	$K_{1\lambda} = 5.5 \times 10^{-3}$ $K_{2\lambda} = -1.0 \times 10^{-3}$
Position Filter	$\Xi_p = 1 \times 10^{-5}I$ $\Xi_a = 1 \times 10^{-5}I$	$\Theta_p = 1I$	$K_{1p} = 8.5 \times 10^{-3}I$ $K_{2p} = 3.2 \times 10^{-3}I$
Linear Estimator	$\Xi_{KF} = 1I$	$\Theta_{KF} = 10^{-5}I$	Time Var.
NonLinear Estimator	$\Xi_{KF} = 1I$	$\Theta_{KF} = 10^{-4}I$	Time Var.

These filters are designed to produce a close-loop frequency response that merges the frequency contents of each sensor. These frequency response can be seen in Fig.6, where the low frequencies of the Compass and GPS are mixed with the high frequencies of the inertial measurements, resulting in a unitary response for the sum of the two transfer functions in each system.

Both systems were tested for stability using Lyapunov method. Let $F_{CL} = (F - KH)$ be the close loop matrix for the (IV-B) where K is the Kalman gain presented in Table V. Solving the Lyapunov discrete equation ($F_{CL}PF_{CL}^T - P + Q = 0$) where Q is used as the main diagonal of the error covariance matrix from the Kalman gain calculation. Is then possible to verify by the definition [12] that the systems are UAS (Uniform Assimptotically Stable).

C. Simulation Results

This section shows the performance of the suggested estimation model in Simulation environment. Due to a limitation already explained, where the model doesn't work with velocities v_x close to 0, all the simulations start with the condition that the car is already moving at a constant $v_x = 10m/s$. Since no real data is involved at this point, a set of inputs, steering angle (δ) and longitudinal force (F_x) is predefined, which includes soft and hard accelerations, braking, long turns,

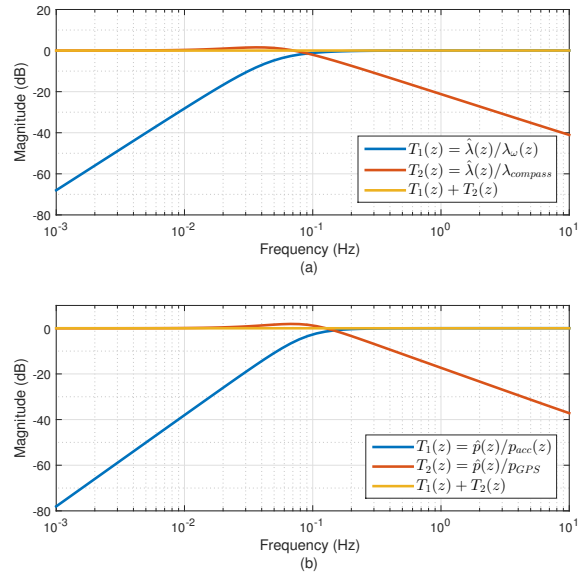


Fig. 6. Complementary filters frequency response. (a) Attitude filter. (b) Position filter

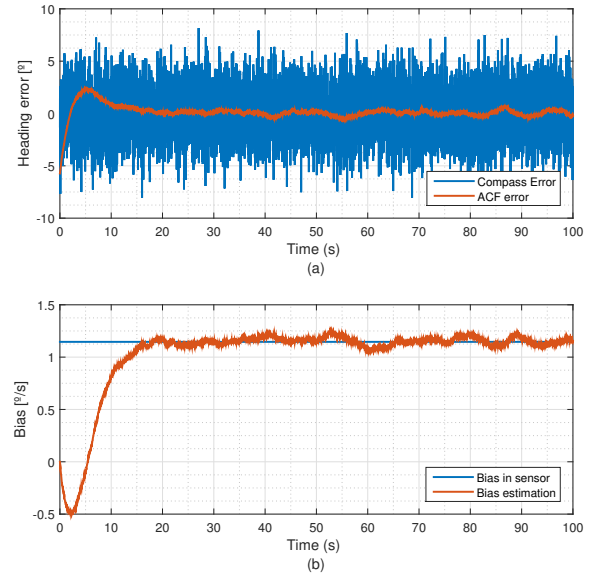


Fig. 7. Heading error compared to true value and bias. (a) Heading error. (b) Bias estimation.

slaloms, and combinations between them. The performance of the ACF can be seen in Fig. 7, where the filter started with $\lambda = -5.73^\circ$ as initial condition. On Fig.7(b) is depicted the bias estimation by the ACF in relation to the constant bias on the sensor.

The position complementary filter starts with initial conditions different from the optimal for two main reasons. The initial position starts with $[p_x \ p_y]^T = [10 \ 4]^T$ since the filter will rarely start in the exact spot where the origin of the global referential was defined. The other is the initial velocity, as explained before, the filter doesn't work for null longitudi-

dinal velocity, so the filter must start with the car already moving, and at this point the velocity is still an unknown, and because of this situation, an initial $[v_x \ v_y]^T = [8 \ 1]^T$ is defined.

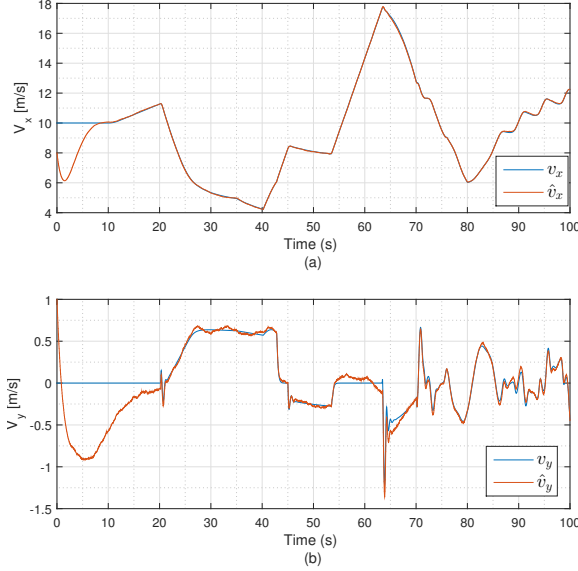


Fig. 8. Theoretical velocity related to the estimated from PCF. (a) Longitudinal velocity v_x . (b) Lateral velocity v_y .

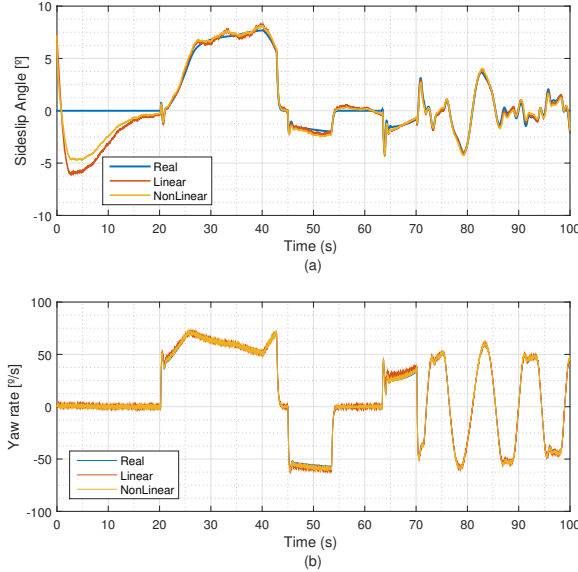


Fig. 9. Theoretical response of the car compared with the Linear and Non-linear models using wet asphalt tyres model (a) Sideslip angle β . (b) Yaw rate $\dot{\psi}$.

The resulting velocity from the PCF is related to the theoretical real velocity in Fig.8, where not only the initial conditions are evident but also the influence of the heading error seen before in the first 15-20seg. For the estimation using the vehicle model (linear and non-linear) with the values from the ACF and PCF, the initial conditions were also defined to

be correspondent with the ones set in PCF. A big unknown in every car model is the tyre, and the forces it can generate for each slip angle. This situation motivated a modification to the simulation model, where the tyres constants were set to wet asphalt as seen in Table I, while the estimation car model uses dry asphalt conditions. The comparison of resulting sideslip angle (β) for the linear and non-linear estimation and for the theoretically real can be seen in Fig.9. This study shows that even when the models are incorrect the proposed filter combination can overcome the difference and still generate a reliable estimation.

V. REAL DATA AND ANALYSIS

Real data was acquired in a test day Fig.10. Rate gyros, compass and accelerometers from a 9dof IMU and GPS data were acquired. The complementary filter to estimate the attitude (ACF) was applied to the real data and the results are shown in Fig.11(a).

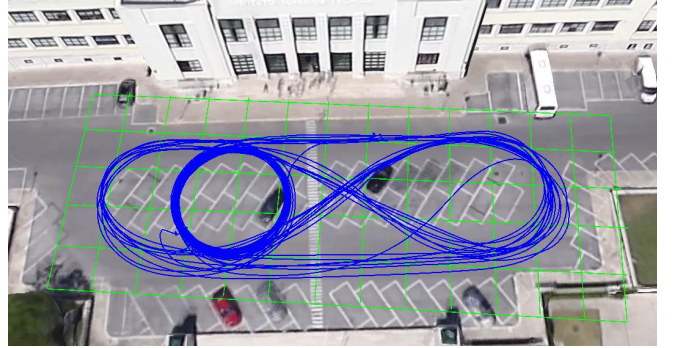


Fig. 10. Trajectory of the car (blue) overlaid with a satellite image using Google Earth. A grid (green) with 5 meters divisions is also present for better notion of space.

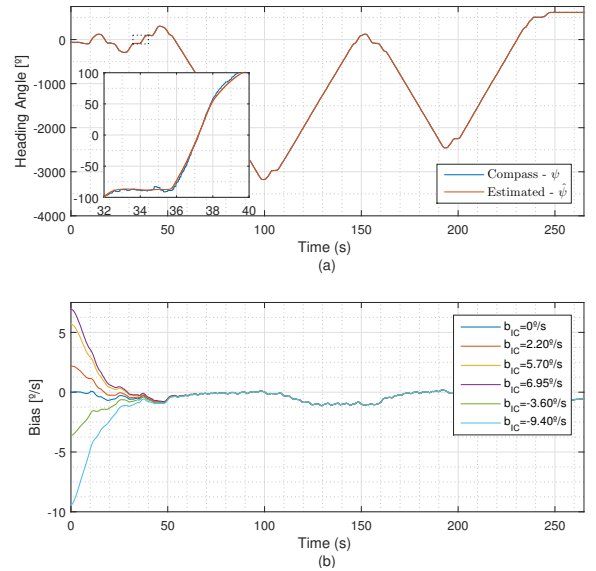


Fig. 11. Heading estimation with real data. (a) Heading comparison between ACF estimation and compass. (b) Bias estimation for several initial conditions.

Results show that the compass data filtered with the gyro data converge to an estimate of the attitude that seems pretty acceptable. Moreover the bias estimation Fig.11(b) shows global stability. In fact whatever is the initial value of the bias, it converges to an average value of -0.5 degrees/s, which is the value already known for this rate gyro.

PCF results are undergoing to fit the estimates to the real position data.

VI. CONCLUSION

An estimator architecture was presented for the estimation of sideslip, using an attitude filter to calculate the car heading relative to a global referential and to estimate the bias on the rate gyro, a position filter to estimate the velocities of the car in the body frame. A Lyapunov stability analysis was performed showing the filters are asymptotically stable. Using the velocities and the bias corrected rate gyro data, two alternative planar models were used to estimate the sideslip of the car, a linear and a non-linear (for comparison purposes). A car dynamics model was developed and the sensors were modeled including stochastic disturbances. Finally, the performance of the proposed methodology was tested with the car dynamic model, using different tyre conditions. The conclusion was that the algorithm could estimate the sideslip of the car within an acceptable error, even when the tyre model was inconsistent between the car dynamic model and the estimator. On the other hand, even with the EKF estimator resulting in an inferior estimation error, the KF estimator didn't stay far behind, and for an hardware implementation the EKF may not justify the complexity and unstablity issues. The ACF was tested with real data providing encouraging results, namely the global stability of the bias estimation. The PCF results will be provided in the near future. The expansion for a 3 dimensional system is planned for the near future, i.e. the implementation of non-null roll and pitch angles in the car dynamic model, and on-board test and validation.

ACKNOWLEDGMENT

This work was supported by FCT, through IDMEC, under LAETA, project UID/EMS/50022/2013.

REFERENCES

- [1] Almeida, L., Azevedo, J., Cardeira, C., Costa, P., Fonseca, P., Lima P., Ribeiro, F., Santos, V., "Mobile Robot Competitions: Fostering Advances in Research, Development and Education in Robotics", CON-TROLO'2000, the 4th Portuguese Conference on Automatic Control, Guimarães – Portugal, October 4-6, 2000, pp. 592-597.
- [2] Afonso, P., J. Azevedo, C. Cardeira, B. Cunha, Pedro Lima, and V. Santos. "Challenges and solutions in an autonomous driving mobile robot competition." In Proceedings of the Controlo Portuguese Conference in Automatic Control, Lisbon. 2006.
- [3] Jacoff, Adam, Elena Messina, Brian A. Weiss, Satoshi Tadokoro, and Yuki Nakagawa. "Test arenas and performance metrics for urban search and rescue robots." In Intelligent Robots and Systems, 2003.(IROS 2003). Proceedings. 2003 IEEE/RSJ International Conference on, vol. 4, pp. 3396-3403. IEEE, 2003.
- [4] J. F. Vasconcelos, B. Cardeira, C. Silvestre, P. Oliveira, P. Batista, "Discrete-Time Complementary Filters for Attitude and Position Estimation: Design, Analysis and Experimental Validation" *IEEE Transactions on Control Systems Technology*, vol. 19, no. 1, pp. 181-198, January 2011.
- [5] Reza N. Jazar, "Vehicle Planar Dynamics" in *Vehicle Dynamics: Theory and Application*, 1st ed. New York:Springer, 2008, ch.10
- [6] M. Abe, "Vehicle Handling Dynamics: Theory and Application", 1st ed., Butterworth-Heinemann publications, 2009, ch2-3, pp.5-117
- [7] U. Kiencke, L. Nielsen, "Wheel Model" in *Automotive Control Systems: For Engine, Driveline, and Vehicle*, 2nd ed. Germany: Springer, ch.8, sec.3 pp314-323
- [8] J. Ryu, E.J. Rossetter, J.C. Gerdes, "Vehicle Sideslip and Roll Parameter Estimation using GPS", in *6th Int. Symposium on Advanced Vehicle Control*, Hiroshima, Symp., 2002
- [9] K. Nam, S. Oh, H. Fujimoto, Y. Hori, "Estimation of Sideslip and Roll Angles of Electric Vehicles Using Lateral Tire Force Sensors Through RLS and Kalman Filter Approaches", in *IEEE Transactions on Industrial Electronics*, Vol.60, No.3, 2013, pp.988-1000
- [10] Gene F. Franklin, J. David Powell, Michael Workman, "Multivariable and Optimal Control" in *Digital Control of Dynamic Systems*, 3rd ed, Ellis-Kagle Press: 2006, ch9, pp389-391
- [11] R. Brown, P. Hwang, "Discrete Kalman Filter Basics" in *Introduction to Random Signals and Applied Kalman Filtering: with Matlab exercises*, 4th ed. New York: Wiley, 2012, ch.7, pp.249-262
- [12] Wilson J. Rugh, "Discrete Time: Lyapunov Stability Criteria", in *Linear System Theory*, 2nd ed. New Jersey: Prentice Hall, 1996, ch.23, pp.437-446